Synthesis of nonlinear robust control for aerial vehicles under parameter uncertainties

Nguyen Viet Phuong[1*], Nguyen Duy Khanh[2]

[1]Institute of Missile, Academy of Military Science and Technology, 17 Hoang Sam, Nghia Do, Hanoi, Vietnam;
[2]Faculty of Industrial Automation and Electrical Engineering, Saint Petersburg Electrotechnical University (LETI), 5 Professor Popova Street, Saint Petersburg, Russia.
[*]Corresponding author: vphuongvtl@gmail.com

Received 10 Mar. 2025; Revised 15 May 2025; Accepted 19 May 2025; Published 25 Aug. 2025.
DOI: https://doi.org/10.54939/1859-1043.j.mst.105.2025.28-35

ABSTRACT

This paper proposes a nonlinear robust control strategy for the longitudinal motion channel of an aerial vehicle (AV) to enhance flight control quality under parameter uncertainties. A mathematical model of the control object is developed, and a robust nonlinear controller is synthesized using sliding mode control (SMC) combined with a reference model. The controller parameters are designed based on Lyapunov stability theory, ensuring the robust stability of the closed-loop system. A linear modal controller is developed to compare with the proposed nonlinear controller. Comparative simulations conducted in MATLAB/Simulink highlight the superior performance of the proposed controller in terms of tracking accuracy and robustness.

Keywords: Aerial vehicle; Robust nonlinear control; Sliding mode control; Longitudinal motion; Parameter uncertainty.

1. INTRODUCTION

Unmanned Aerial Vehicles (UAVs) have emerged as critical platforms for applications ranging from surveillance and logistics to disaster response and military operations. The dynamic and often unpredictable environments in which UAVs operate necessitate robust control systems capable of ensuring stability and precise tracking under uncertainties, such as aerodynamic parameter variations and external disturbances. Longitudinal motion control, which governs pitch angle and angular velocity, is particularly vital for maintaining stable flight and achieving accurate trajectory tracking in UAVs. However, parameter uncertainties arising from modeling inaccuracies or environmental factors pose significant challenges to conventional control strategies.

Recent advancements in nonlinear control techniques, particularly Sliding Mode Control (SMC), have shown promise in addressing these challenges due to their robustness against uncertainties and disturbances [1, 2]. SMC operates by driving system states onto a sliding surface and maintaining them there, ensuring stable and accurate tracking. Studies have demonstrated the effectiveness of SMC in UAV applications, including attitude control under complex disturbances [3] and formation control with adaptive mechanisms [4]. Additionally, integrating SMC with reference models or disturbance observers has improved transient response and tracking accuracy [5, 6]. Despite these developments, many existing SMC-based controllers focus on simplified UAV models or neglect realistic aerodynamic uncertainties, limiting their applicability to small-scale UAVs like the UAV-70V considered in this study, which are highly sensitive to parameter variations due to their lightweight structures [7].

This paper proposes a robust nonlinear control strategy for the longitudinal motion of a UAV under parameter uncertainties, synthesized using SMC combined with a reference model. By leveraging Lyapunov stability theory, the controller ensures robustness against bounded aerodynamic uncertainties while achieving high tracking performance. Comprehensive simulations on the UAV-70V model using MATLAB/Simulink demonstrate the controller's superior performance in terms of overshoot, settling time, and tracking error compared to a linear modal controller. This work advances UAV control by offering a practical solution tailored to small-scale aerial vehicles, addressing the gap in robust control for longitudinal motion under realistic uncertainties and providing insights for real-world implementation.

2. SYNTHESIS OF AERIAL VEHICLE CONTROL SYSTEM

In figure 1, the following coordinate systems are used: x_0Oy_0: Ground coordinate system; x_aOy_a: Velocity coordinate system; x_kOy_k: Link coordinate system.

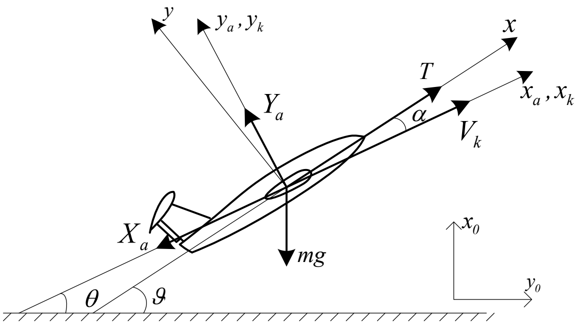

Figure 1. *Longitudinal motion model of the aerial vehicle.*

The mathematical model of the longitudinal motion of the aerial vehicle is expressed as [8]:

$$\begin{cases} m\dot{V}(t) = T\cos\alpha - X_a - mg\sin\theta; \\ mV\dot{\theta}(t) = T\sin\alpha + Y_a - mg\cos\theta; \\ J_z\dot{\omega}_z = qSbm_z;\ \dot{\vartheta} = \omega_z; \\ \dot{x}(t) = V\cos\theta; H(t) = V\sin\theta, \end{cases} \tag{1}$$

Where: ϑ, θ, α - Pitch angle, trajectory inclination angle, and angle of attack of the aerial vehicle. V- Velocity of the aerial vehicle; mg - Gravitational force of the aerial vehicle; T - Engine thrust force; S - Characteristic area of the aerial vehicle; J_z - Moment of inertia about the z-axis; q - Dynamic pressure; *x*, H - Coordinates of the center of mass of the aerial vehicle in the ground coordinate system; X_a, Y_a - Components of the drag and lift forces, respectively; m_z - Moment coefficient about the z-axis; b - Average aerodynamic chord length.

The system of differential equations based on small deviations is obtained:

$$\begin{cases} \dot{\alpha}(t) = \omega_z(t) + a_y^{\alpha}\alpha(t) - a_y^{\delta_c}\delta_c; \\ \dot{\omega}_z(t) = -a_{m_z}^{\alpha}\ \alpha(t) - a_{m_z}^{\omega_z}\omega_z(t) - a_{m_z}^{\delta_c}\delta_c;\ \dot{\vartheta}(t) = \omega_z(t). \end{cases} \tag{2}$$

Where: δ_c - Deflection angle of the aerial vehicle's control surface; a_y^{α} , $a_y^{\delta_c}$, $a_{m_z}^{\alpha}$, $a_{m_z}^{\omega_z}$, $a_{m_z}^{\delta_c}$ are the flight dynamics coefficients.

2.1. Robust sliding mode control with reference model

To design the robust nonlinear controller, system (2) is reformulated as follows:

$$\begin{cases} \dot{\vartheta} = \omega_z;\ \dot{\omega}_z = a_1\omega_z + a_2\alpha + b_1u + d_1(\omega_z,\alpha,u); \\ \dot{\alpha} = \omega_z + a_3\alpha + b_2u + d_2(\alpha,u); \end{cases} \tag{3}$$

Where $u = \delta_c$; $a_1 = -a_{m_z}^{\omega_z}$; $a_2 = -a_{m_z}^{\alpha}$; $a_3 = a_y^{\alpha}$; $b_1 = -a_{m_z}^{\delta_c}$; $b_2 = -a_y^{\delta_c}$; $d_1(\omega_z,\alpha,u)$ and $d_2(\alpha,u)$ – Represent the uncertain components caused by parameter uncertainties of the object.

Assume that $|d_1| \le D_1$, $|d_2| \le D_2$ (D_1 and D_2 – Positive constants).

A reference model is introduced with dynamics designed as follows:

$$\dot{\mathbf{X}}_m = \mathbf{A}_m \mathbf{X}_m + \mathbf{B}_m r \tag{4}$$

Where $\mathbf{A}_m$, $\mathbf{B}_m$ is designed such that the system (4) is stable and satisfies the desired control performance metrics; r is the desired output value.

The control objective is to design a robust controller such that $\|\mathbf{X} - \mathbf{X}_m\| \le \varepsilon$ with ε is a very small permissible error, $\mathbf{X}_m = \begin{bmatrix} \vartheta_d & \omega_{zd} & \alpha_d \end{bmatrix}^{\mathrm{T}}$ is the desired state vector; $\mathbf{X} = \begin{bmatrix} \vartheta & \omega_z & \alpha \end{bmatrix}^{\mathrm{T}}$ is the state vector of the object.

Define the tracking error as $e_1 = \vartheta - \vartheta_d$; $e_2 = \omega_z - \omega_{zd}$; $e_3 = \alpha - \alpha_d$. Combining with system (3), the following system is obtained:

$$\begin{cases} \dot{e}_1 = e_2;\ \dot{e}_2 = a_1 e_2 + a_2 e_3 + b_1 u + \Delta_1 + d_1; \\ \dot{e}_3 = e_2 + a_3 e_3 + b_2 u + \Delta_2 + d_2. \end{cases} \tag{5}$$

Where $\Delta_1 = a_1 \omega_{zd} + a_2 \alpha_d - \dot{\omega}_d$ and $\Delta_2 = \omega_{zd} + a_2 \alpha_d - \dot{\alpha}_d$ can be obtained from system (4).

Next, the robust controller is synthesized [9] as follows:

Let $s = c_1 e_1 + c_2 e_2 + c_3 e_3$ be the sliding surface c_1, c_2, c_3 is a parameter matrix to be designed later. It is clear that $\dot{s} = c_1 \dot{e}_1 + c_2 \dot{e}_2 + c_3 \dot{e}_3$. Combining with system (5), the following equation is obtained:

$$\dot{s} = \left(c_1 + c_2 a_1 + c_3\right) e_2 + \left(c_2 a_2 + c_3 a_3\right) e_3 + \left(c_2 b_1 + c_3 b_2\right) u + \left(c_2 \Delta_1 + c_3 \Delta_2\right) + \left(c_2 d_1 + c_3 d_2\right)$$

A Lyapunov function is chosen as $V_1 = s^2/2$. Its time derivative is $\dot{V}_1 = s\dot{s}$. To ensure $\dot{V}_1 < 0$ the control law is selected as follows:

$$u = -\frac{\left(c_1 + c_2 a_1 + c_3\right) e_2 + \left(c_2 a_2 + c_3 a_3\right) e_3 + \left(c_2 \Delta_1 + c_3 \Delta_2\right) + ks + (\eta + \rho)\operatorname{sign} s}{c_2 b_1 + c_3 b_2} \tag{6}$$

Where $k, \rho > 0$; $\eta \ge |c_2 D_1| + |c_3 D_2| > 0$. Thus

$$\dot{V} = s\left[-ks + c_2 d_1 + c_3 d_2 - (\eta + \rho)\operatorname{sign} s\right],$$

$$\dot{V} \le -ks^2 + \left(c_2 d_1 + c_3 d_2 - |c_2 D_1| - |c_3 D_2|\right)|s| - \rho|s| \le -ks^2 - \rho|s| \le 0.$$

From this, it follows that there exists a time t_0 such that for $t > t_0$, $s = 0$. In equation (6), the parameters $k, \rho > 0$ are chosen arbitrarily; The larger they are, the faster s converges to 0. Next, the parameters c_1, c_2, c_3 must be designed to achieve the control objective.

Choose $c_3 = 1$, so when $t > t_0$, $s = 0$, we have $e_3 = -c_1 e_1 - c_2 e_2$. Substituting into the error dynamics, equation (6) simplifies to:

$$u = -\frac{\left(-c_1 c_2 a_2 - c_1 a_3\right) e_1 + \left(c_1 + c_2 a_1 + 1 - c_2^2 a_2 - c_2 a_3\right) e_2 + c_2 \Delta_1 + \Delta_2}{c_2 b_1 + b_2} \tag{7}$$

Combining (5) and (7), the following system is obtained:

$$\begin{cases} \dot{e}_1 = e_2; \\ \dot{e}_2 = k_1 e_1 + k_2 e_2 + d. \end{cases} \tag{8}$$

Where

$$\begin{cases} k_1 = -a_2c_1 + \dfrac{b_1\left(c_1c_2a_2 + c_1a_3\right)}{c_2b_1 + b_2}; \\ k_2 = a_1 - a_2c_2 - \dfrac{b_1\left(c_1 + c_2a_1 + 1 + c_2^2a_2 - c_2a_3\right)}{c_2b_1 + b_2}; d = -\dfrac{b_1\left(c_2\Delta_1 + \Delta_2\right)}{c_2b_1 + b_2} + \Delta_1 + d_1. \end{cases} \tag{9}$$

Rewriting (8) in matrix form:

$$\dot{\mathbf{E}} = \mathbf{AE} + \boldsymbol{\xi}. \tag{10}$$

Where $\mathbf{E} = \left[e_1 \ e_2\right]^{\mathrm{T}}$; $\mathbf{A} = \left[0 \ 1; k_1 \ k_2\right]$; $\boldsymbol{\xi} = \left[0 \ d\right]^{\mathrm{T}}$. It is evident that systems (8) and (10) are stable if the parameters are designed such that the matrix **A** is Hurwitz. Indeed, consider the Lyapunov function: $V_2 = \mathbf{E}^{\mathrm{T}}\mathbf{PE}$.

Where $\mathbf{P} = \mathbf{P}^{\mathrm{T}} > 0$ – positive definite matrix. Using (10), the time derivative of V_2 is:

$$\dot{V}_2 = \mathbf{E}^{\mathrm{T}}\left(\mathbf{A}^{\mathrm{T}}\mathbf{P} + \mathbf{PA}\right)\mathbf{E} + 2\mathbf{E}^{\mathrm{T}}\mathbf{P}\boldsymbol{\xi}.$$

Let $\mathbf{Q} = \mathbf{Q}^{\mathrm{T}} > 0$ be a positive definite matrix, satisfying the Lyapunov equation $\mathbf{A}^{\mathrm{T}}\mathbf{P} + \mathbf{PA} = -\mathbf{Q}$. Assume $\|\boldsymbol{\xi}\| \le \mu,$ where $\mu > 0$ is a positive constant. Then:

$$\dot{V}_2 \le -\|\mathbf{E}\|\left[\lambda_{\min}(\mathbf{Q})\|\mathbf{E}\| - 2\lambda_{\max}(\mathbf{P})\mu\right].$$

Thus, $\dot{V}_2 < 0$ outside a compact set $G = \left\{\mathbf{E} \mid \|\mathbf{E}\| \le 2\mu\lambda_{\max}(\mathbf{P}) / \lambda_{\min}(\mathbf{Q})\right\}$, meaning $\|\mathbf{E}\|$ is bounded and converges to an invariant set *G* with an adjustable size. In other words, the upper bound of $\|\mathbf{E}\|_\infty$ can be made arbitrarily small by increasing the eigenvalues of the matrix $(-\mathbf{A})$ or ensuring the eigenvalues of the Hurwitz matrix **A** are further to the left of the imaginary axis [10].

We will design the eigenvalues of the matrix **A** to have the values $-\omega_{01}$ and $-\omega_{02}$ where $\omega_{0i} > 0, i = \overline{1,2}.$ It is clear that the larger ω_{0i} are, the further the eigenvalues of **A** are from the imaginary axis toward the left, and $\|\mathbf{E}\|$ converges closer to the neighborhood of 0, or equivalently $e_1; e_2; e_3$ converges closer to the neighborhood of 0. We have the following equation:

$$\det\left|\mathbf{A} - \lambda\mathbf{E}\right| = \begin{vmatrix} -\lambda & 1 \\ k_1 & k_2 - \lambda \end{vmatrix} = \left(\lambda + \omega_{01}\right)\left(\lambda + \omega_{02}\right) \rightarrow \begin{cases} k_1 = -\omega_{01}\omega_{02}; \\ k_2 = -\left(\omega_{01} + \omega_{02}\right). \end{cases}$$

This is the condition to solve for the first two equations of (9) and find c_1, c_2 as follows:

$$\begin{cases} c_2 = \dfrac{-\omega_{01}\omega_{02}b_1b_2}{-a_2b_2 + b_1a_3 + \left(\omega_{01} + \omega_{02}\right)b_1 + \omega_{01}\omega_{02}b_1^2 / \left(-a_2b_2 + b_1a_3\right)}; \\ c_1 = -\omega_{01}\omega_{02}\left(b_1c_2 + b_2\right) / \left(-a_2b_2 + b_1a_3\right). \end{cases} \tag{11}$$

Choose $\omega_{01} = 25;$ $\omega_{02} = 1,$ substitute into (11), then add some direct values such as: $c_1 = 40.7627;$ $c_2 = 1.7219;$ $c_3 = 1.$ The remaining controller parameters are chosen as follows:

$$\mathbf{A}_m = \begin{bmatrix} 0 & 1 & 0 \\ -100.215 & -20 & 0.172 \\ -0.2733 & 0.95 & -1.06 \end{bmatrix}; \ \mathbf{B}_m = \begin{bmatrix} 0 \\ 100.215 \\ 0.2733 \end{bmatrix}; \ K = 10; \ \eta = \rho = 100.$$

2.2. Modal linear control

Modal control is a linear state feedback, given in the following form:

$$u_l = g(t)\cdot\beta + \mathbf{k}^{\mathrm{T}}\mathbf{x} = g(t)\cdot\beta + k_1\alpha + k_2\omega_z + k_3\vartheta, \tag{12}$$

Where: $g(t)$ - Desired reference signal, β - Gain coefficient, $\mathbf{k} = \begin{bmatrix} k_1 & k_2 & k_3 \end{bmatrix}^{\mathrm{T}}$ - A real vector of the feedback coefficients for the state variables, calculated based on the desired location of the poles of the characteristic equation of a closed-loop system. The characteristic polynomial of the closed-loop system (2), (12):

$$\varphi_{\mathrm{dt}}(\lambda) = \det\left(\mathbf{A} + \mathbf{B}\mathbf{k}^{\mathrm{T}} - \lambda\mathbf{E}\right) \tag{13}$$

where **A**, **B** are the state and control matrices in the discrete system (2) and **k** is the control gain matrix. **E** - Identity matrix.

By substituting the matrices **A** and **B**, equation (13) is rewritten as follows:

$$\begin{aligned}\varphi_{dt}(\lambda) &= -\lambda^3 + \left(a_y^{\alpha} - a_{m_z}^{\omega_z} - a_y^{\delta_c}k_1 - a_{m_z}^{\delta_c}k_2\right)\lambda^2 + \\ &\left[-\left(a_{m_z}^{\delta_c} + a_{m_z}^{\omega_z}a_y^{\delta_c}\right)k_1 + \left(a_y^{\alpha}a_{m_z}^{\delta_c} + a_{m_z}^{\alpha}a_y^{\delta_c}\right)k_2 - a_{m_z}^{\delta_c}k_3 - a_{m_z}^{\alpha} + a_y^{\alpha}a_{m_z}^{\omega_z}\right]\lambda + \\ &+\left(a_y^{\alpha}a_{m_z}^{\delta_c} + a_{m_z}^{\alpha}a_y^{\delta_c}\right)k_3.\end{aligned} \tag{14}$$

Select the characteristic polynomial for the linearized closed-loop system (2), (12) as

$$\begin{aligned}\varphi_{mm}(\lambda) &= -(\lambda+\omega_1)(\lambda+\omega_2)(\lambda+\omega_3) \\ &= -\lambda^3 + (\omega_1+\omega_2+\omega_3)\lambda^2 + (-\omega_1\omega_2 - \omega_1\omega_3 - \omega_2\omega_3)\lambda + \omega_1\omega_2\omega_3\end{aligned} \tag{15}$$

The roots of it are multiples of negative real numbers in the form:

$$\lambda_1 = -\omega_1, \lambda_2 = -\omega_2, \lambda_3 = -\omega_3$$

By equating coefficients of equal degree in polynomials (14) and (15), the algebraic system for determining the feedback coefficients $\mathbf{k} = \begin{bmatrix} k_1 & k_2 & k_3 \end{bmatrix}^{\mathrm{T}}$ is obtained as follows:

$$\begin{cases} a_y^{\alpha} - a_{m_z}^{\omega_z} - a_y^{\delta_c}k_1 - a_{m_z}^{\delta_c}k_2 = \omega_1 + \omega_2 + \omega_3; \\ -\left(a_{m_z}^{\delta_c} + a_{m_z}^{\omega_z}a_y^{\delta_c}\right)k_1 + \left(a_y^{\alpha}a_{m_z}^{\delta_c} + a_{m_z}^{\alpha}a_y^{\delta_c}\right)k_2 + \\ -a_{m_z}^{\delta_c}k_3 - a_{m_z}^{\alpha} + a_y^{\alpha}a_{m_z}^{\omega_z} = -\omega_1\omega_2 - \omega_1\omega_3 - \omega_2\omega_3; \left(a_y^{\alpha}a_{m_z}^{\delta_c} + a_{m_z}^{\alpha}a_y^{\delta_c}\right)k_3 = \omega_1\omega_2\omega_3. \end{cases} \tag{16}$$

From (2) the following transfer function is obtained:

$$W_{\vartheta}^{\delta_c} = \frac{a_{m_z}^{\delta_c}s - \left(a_{m_z}^{\delta_c}a_y^{\alpha} + a_y^{\delta_c}a_{m_z}^{\alpha}\right)}{s^3 + \left(a_{m_z}^{\omega_z} - a_y^{\alpha}\right)s^2 + \left(a_{m_z}^{\alpha} - a_y^{\alpha}a_{m_z}^{\omega_z}\right)s}$$

Since the transfer function $W_{\vartheta}^{\delta_c}$ has a single zero at $s = -1.06$, the desired poles of the control system are chosen such that $\lambda_1 = -\omega_1 = -1.06;$ $\lambda_2 = -\omega_2 = -15;$ $\lambda_3 = -\omega_3 = -15.$ From this, by using formulas (15) and (16) the value of the feedback coefficient vector of the modal controller can be obtained as $\mathbf{k} = \begin{bmatrix} -0.4823 & 0.8728 & 6.8328 \end{bmatrix}^{\mathrm{T}}$. The gain coefficient is: $\beta = \left[-\mathbf{C}\left(\mathbf{A}+\mathbf{B}\mathbf{k}\right)^{-1}\mathbf{B}\right]^{-1} = -6.8328.$

3. RESULTS AND DISCUSSION

In this section, the control object chosen for the simulation is the UAV-70V. The UAV has the following basic parameters: a length of 2707 mm, a weight of 56.3 kg, a wing area of 1.05 m², and a wingspan of 3000 mm. The average aerodynamic chord is 350 mm, and the cruising speed is 40 m/s. Additionally, the moment of inertia of the UAV is 31.3 kg·m². The simulation of the UAV's reference signal tracking is investigated with the aerodynamic coefficients [11] in the 4 parameter scenarios (tentatively called scenarios a_1, a_2, a_3, a_4 shown in table 1) when using different controllers. The case of nominal parameters is scenario a_1.

Table 1. *Aerodynamic parameters of the aerial vehicle.*

Parameter / Scenario	$a_y^{\alpha}\,(s^{-1})$	$a_{m_z}^{\alpha}\,(s^{-2})$	$a_{m_z}^{\omega_z}\,(s^{-1})$	$a_y^{\delta_c}\,(s^{-1})$	$a_{m_z}^{\delta_c}\,(s^{-2})$
a_1	-1.10	15.5	1.20	0.09	33.0
a_2	-0.86	5.81	0.18	0.06	9.15
a_3	-1.34	-12.5	0.45	0.07	15.2
a_4	-1.25	-37.5	0.12	0.08	9.3

The simulation results are shown in figures 2-4, where "RSMC" – Proposed Robust Sliding Mode Control; "Modal" – Modal Linear Control; "Desired" – Desired Signal.

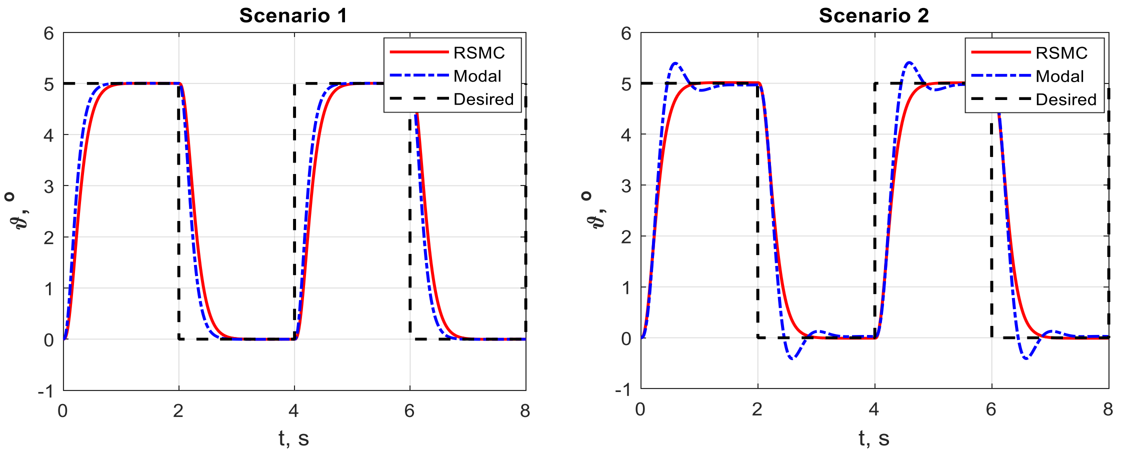

Figure 2. *Response of the pitch angle ϑ to a square wave signal in scenarios a_1 and a_2.*

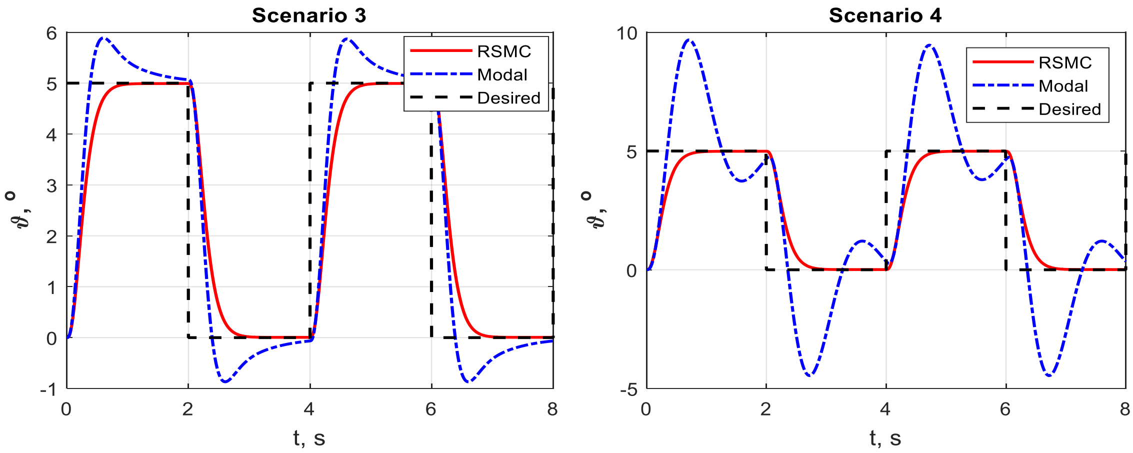

Figure 3. *Response of the pitch angle ϑ to a square wave signal in scenarios a_3 and a_4.*

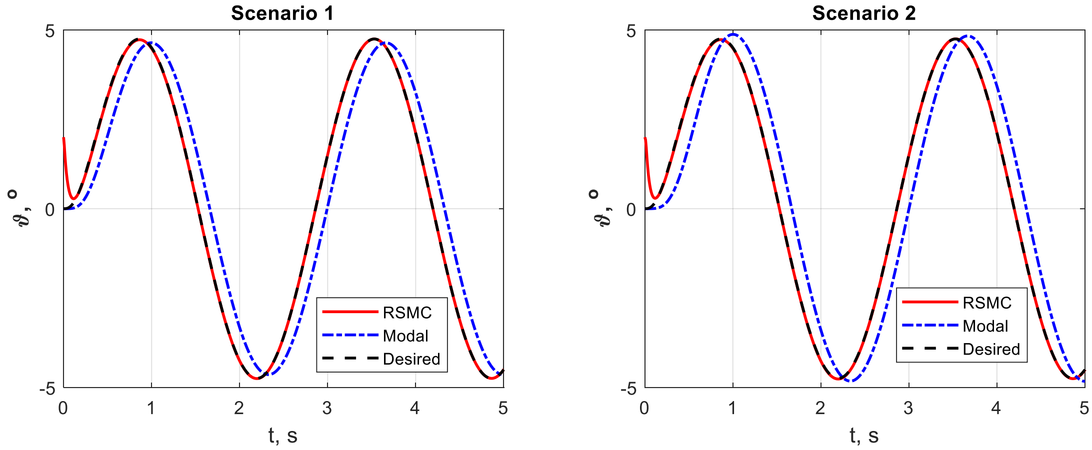

Figure 4. *Response of the pitch angle ϑ to a sinusoidal signal in 4 scenarios a_1 and a_2.*

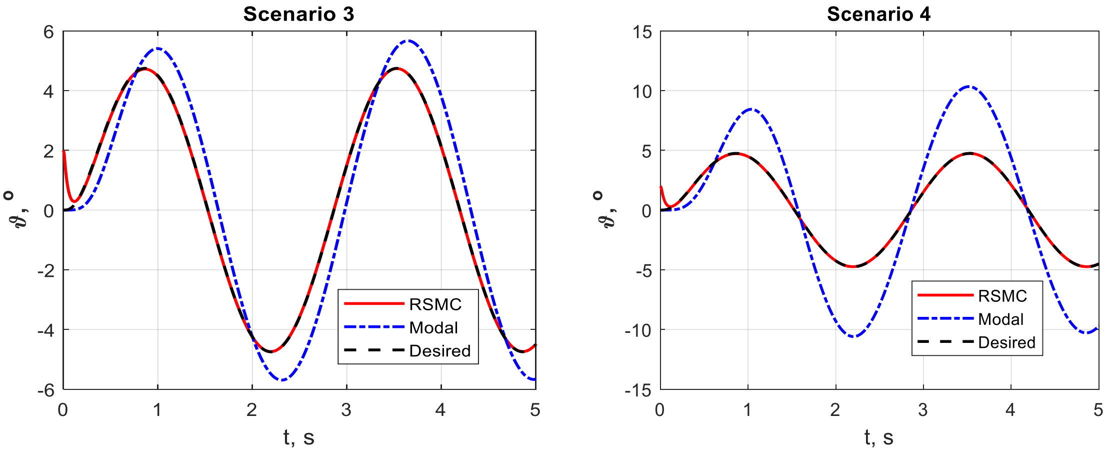

Figure 5. *Response of the pitch angle ϑ to a sinusoidal signal in 4 scenarios a_3 and a_4.*

Observations:

- Figures 2 and 3 show that the linear modal controller performs well under nominal conditions (no overshoot, settling time ~0.5 s). However, under parameter variations, its performance degrades, with overshoot exceeding 10% and settling time greater than 1 s, potentially leading to instability in extreme cases. In contrast, the SMC controller maintains excellent performance (0% overshoot, 0.5 s settling time) across all scenarios.

- Figures 4 and 5 demonstrate that the SMC controller closely tracks sinusoidal reference signals, achieving high stability and control quality under parameter variations. The linear modal controller fails to track sinusoidal signals accurately, with noticeable tracking errors and potential instability.

4. CONCLUSIONS

This paper proposes a nonlinear robust control system for the longitudinal motion of a UAV under parameter uncertainties, synthesized using SMC combined with a reference model. The controller parameters are derived based on Lyapunov stability theory, ensuring robust stability against bounded uncertainties. The tracking error can be made arbitrarily small by tuning the controller parameters. Comparative simulations with a linear modal controller validate the superior performance of the proposed SMC controller, consistent with theoretical analyses. Future work will explore higher-order SMC to reduce chattering and real-world implementation on the UAV-70 V platform.

REFERENCES

[1]. S. Sui, Y. Yao, and F. Zhu, *"An anti-disturbance attitude control method for fixed-wing unmanned aerial vehicles based on an integral sliding mode under complex disturbances during sea flight,"* Drones, vol. 9, no. 3, p. 164, (2025), doi: 10.3390/drones9030164.

[2]. M. Xie and H. Ren, *"Formation control of unmanned aerial vehicles based on cooperative sliding mode adaptive control,"* Int. Core J. Eng., vol. 11, no. 4, pp. 196–206, (2025), doi: 10.6919/ICJE.202504_11(4).0022.

[3]. A. K. Khotimah et al., *"Control strategy of unmanned aerial vehicle (UAV) by using sliding mode control method,"* J. Phys.: Conf. Ser., vol. 2719, p. 012042, (2024), doi: 10.1088/1742-6596/2719/1/012042.

[4]. Y. Wang et al., *"Fixed-time neuro-sliding mode controller design for quadrotor UAV transporting a suspended payload,"* Neurocomputing, vol. 492, pp. 147–160, (2023), doi: 10.1016/j.neucom.2023.04.056.

[5]. L. A. Alsafadi and I. V. Mironova, *"Sliding mode controller design for unmanned aerial vehicles with unmodeled polytopic dynamics,"* IFAC-PapersOnLine, vol. 54, no. 21, pp. 204–209, (2021), doi: 10.1016/j.ifacol.2021.10.486.

[6]. R. Shrestha, I. Oh, and S. Kim, *"A survey on operation concept, advancements, and challenging issues of urban air traffic management,"* Drones, vol. 7, no. 2, p. 89, (2023), doi: 10.3390/drones7020089.

[7]. Y. Zhang and J. Liu, *"Integrating artificial intelligence and control systems for autonomous platforms: A review,"* IEEE Trans. Ind. Informat., vol. 19, no. 6, pp. 3048–3058, (2023), doi: 10.1109/TII.2022.3206543.

[8]. Соколов, Д. М. *"Аэродинамические характеристики БПЛА при маневрировании на малых высотах,"* Труды СПбПУ, т. 529, № 1, стр. 78–92, (2023), doi: 10.18721/JEST.52901.

[9]. X. Rong and U. Ozguner, *"Sliding mode control of a class of underactuated systems,"* Automatica, vol. 44, pp. 233–248, (2008), doi: 10.1016/j.automatica.2007.05.014.

[10]. H. K. Khalil, *"Nonlinear Systems",* 3rd ed., Englewood Cliffs, NJ: Prentice-Hall, (2002), 750p.

[11]. V. F. Nguen, A. V. Putov, and T. T. Nguen, *"Adaptive control of an unmanned aerial vehicle,"* in Proc. AIP Conf., vol. 1798, no. 020124, pp. 020124-1–020124-11, (2017), doi: 10.1063/1.4972716.

TÓM TẮT

Tổng hợp điều khiển phi tuyến bền vững cho thiết bị bay với tham số bất định

Bài báo đề xuất bộ điều khiển phi tuyến bền vững cho kênh chuyển động dọc của thiết bị bay với mục tiêu nâng cao chất lượng điều khiển bay trong điều kiện tham số đối tượng bất định. Trong đó xây dựng mô hình toán học của đối tượng điều khiển. Bộ điều khiển phi tuyến bền vững được tổng hợp dựa trên thuật toán điều khiển trượt kết hợp với mô hình tham chiếu. Các tham số của bộ điều khiển đề xuất được thiết kế dựa trên phương pháp hàm Lyapunov, từ đó chứng minh tính ổn định bền vững của hệ thống kín. Bộ điều khiển tuyến tính modal được xây dựng để so sánh với bộ điều khiển phi tuyến bền vững. Kết quả mô phỏng trên phần mềm MATLAB/Simulink đã chứng minh tính hiệu quả của bộ điều khiển đề xuất.

Từ khóa: Thiết bị bay; Điều khiển phi tuyến bền vững; Điều khiển trượt; Chuyển động dọc; Tham số bất định.